Journal of Structural Geology, Vol. 13, No. 10, pp. 1173 to 1183, 1991
Printed in Great Britain

0191-8141/91 $03.00+0.00

Conditions of vein formation in the southern Appalachian foreland: constraints from vein geometries and fluid inclusions

J. LINCOLN FOREMAN* and WILLIAM M. DUNNE

Department of Geological Sciences, University of Tennessee, Knoxville, TN 37996-1410, U.S.A.

(*Received* 20 *August* 1990; *accepted in revised form* 15 *May* 1991)

Abstract—The Nolichucky Shale in the Whiteoak Mountain thrust sheet of the southern Appalachian foreland contains four coeval bed-normal calcite vein sets that trended 015°, 055°, 090° and 320° before thrusting. The pre-tectonic veins were displaced by syn-tectonic bed-parallel slickensided calcite veins during local Alleghanian thrusting. Fluid inclusion thermometry indicates precipitation of both bed-normal and bed-parallel veins from NaCl–$CaCl_2$ brines (27 wt% NaCl-equiv. salinity), at 80–110°C for bed-normal veins and 110°C for bed-parallel veins. These temperatures correspond to burial depths of 2.4–3.6 km, which were attained after the middle Mississippian. These pressure-corrected homogenization temperatures are comparable to time–temperature indicators, such as CAI and illite crystallinity, and indicate that inclusions were trapped near-maximum burial conditions and were not deformed after trapping. This conclusion is supported by the absence of petrographic evidence for inclusion failure and a worst-case mechanical analysis that indicates a lack of brittle deformation to inclusions after trapping.

The four coeval bed-normal vein sets could not be formed by one simple stress field, nor by the development of a single structure, but required the interaction of at least two stress components or structures. It is proposed that the interaction of the Alleghanian and Ouachita orogenic stress components, beyond the limits of thrusting, produced the sets as coeval Alleghanian orthogonal (055°, 320°) and Ouchita sub-orthogonal (015°, 090°) mode I fractures.

INTRODUCTION

THE great abundance of bed-normal joints and veins within foreland thrust sheets reflects the diverse mechanisms that can produce these fractures before, during or after thrusting. Before thrusting, they may develop in response to regional stress fields unrelated to tectonic stress buildup prior to thrusting (Nickelsen & Hough 1967, Dunne 1986, Kilsdonk & Wiltschko 1988). During thrusting, bed-normal and bed-oblique fractures are localized in buckle folds or by passage through ramps (Price 1967, Srivastava & Engelder 1990). Following thrusting, bed-normal fractures can develop in rocks that are nearly horizontal. Fracture trends can be controlled by waning orogenic compression, residual tectonic stress, contemporary stress field or rock fabric (Engelder 1985, Hancock & Engelder 1989, Dunne & North 1990). Consequently, bedding-normal geometry does not uniquely constrain fracture initiation with respect to thrust sheet formation. Other constraints such as cross-cutting relationships of fractures, or environmental conditions (pressure, temperature, fluid composition) derived from geochemical data are required to constrain timing (Hancock 1985, Kilsdonk & Wiltschko 1988, Srivastava & Engelder 1990). In this paper, we discuss (1) the use of fracture analysis and fluid inclusion data to elucidate timing relationships between bed-normal veins, bed-parallel veins, and thrust sheet emplacement, and (2) possible pre-thrusting regional controls on bed-normal vein geometries in the southern Appalachians.

GEOLOGIC SETTING

Bed-normal and bed-parallel calcite veins from the Upper Cambrian Nolichucky Shale were examined in outcrop and drill core on the U.S. Department of Energy Oak Ridge Reservation (ORR) near Oak Ridge, Tennessee (Fig. 1a). The Nolichucky Shale is about 175 m thick and consists of approximately 75% dark brown to dark green shale, and interbedded 0.3–1.0 m thick, laterally discontinuous limestones with less abundant calcareous siltstones.

The study area is located in the Whiteoak Mountain (WOM) thrust sheet of the southern Appalachian foreland thrust system (Fig. 1b). The WOM sheet formed during the foreland propagation of the thrust system in the Alleghanian orogeny. The sheet overlies the younger Kingston thrust sheet and is overlain by the older Copper Creek thrust sheet (Fig. 1b). The basal thrust for the WOM sheet is in the Lower Cambrian Rome Formation, the regional detachment of the foreland thrust system in the southern Appalachians (Rich 1934, Rodgers 1949). Field mapping and balanced cross-sections across the WOM sheet (Milici 1970, Woodward 1985, J. Hopson personal communication) show that the sampled Nolichucky Shale is above a footwall ramp (Fig. 1b) and moved through a lower fault-bend fold during thrusting.

Within the study area, the Nolichucky Shale has a consistent bedding orientation of 055/50SE as part of a hangingwall panel above a footwall ramp. Folds in

*Present address: Exxon Production Research Co., P.O. Box 2189, Room ST-4209, Houston, TX 77252-2189, U.S.A.

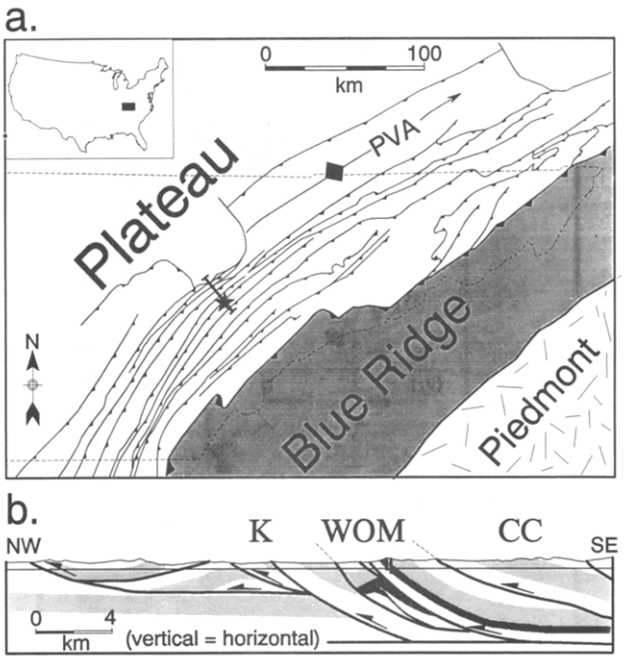

Fig. 1. Structural map and balanced section. (a) Oak Ridge Reservation (star) is located in the foreland of the Valley and Ridge Province (clear pattern). PVA = Powell Mountain anticline; heavy lines with teeth = thrust faults; thin dashed line = Tennessee state boundary. (b) Balanced cross-section through Whiteoak Mountain (WOM) sheet showing position of Nolichucky Shale (dark stipple) and Cambro-Ordovician Knox Group (light stipple). Vertical lines = well locations; K = Kingston thrust sheet; CC = Copper Creek thrust sheet. Modified from Milici (1970), Woodward (1985) and J. Hopson (personal communication).

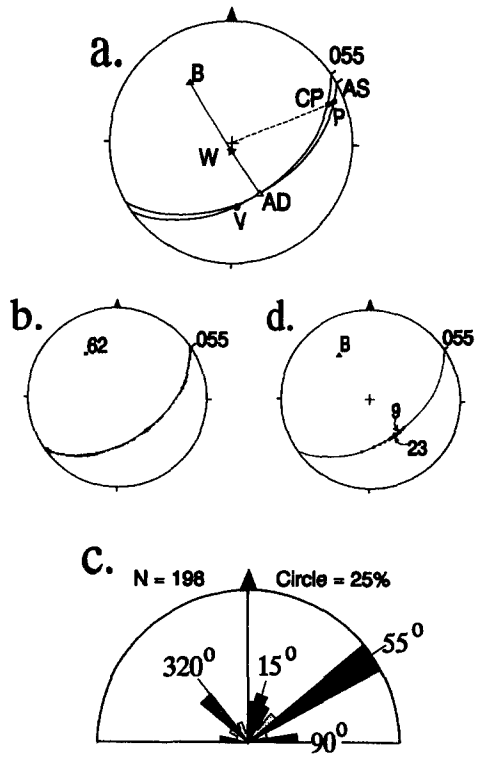

Fig. 2. (a) Equal-area lower hemisphere stereographic projection (stereonet) for correcting pitch of bed-normal vein trace on bedding. B = bedding pole; W = well plunge; AD = apparent dip of bedding; V = vein pole; P = measured pitch; CP = corrected pitch; AS = apparent strike; 055 = bedding strike. (b) Stereonet for bed-normal and bed-parallel veins (62 = number of measured bed-parallel veins; 198 measured bed-normal veins). (c) Rose diagram for azimuths of bed-normal veins after bedding has been rotated to horizontal. Numbers are azimuths of prominent vein sets. (d) Stereonet showing 62 slickenside trends on the bedding trace (B—bedding pole, 9 and 23—number of locally clustered measurements on net).

Nolichucky Shale cores are rare and have amplitudes of less than 1 m. The only faults are rare shear veins with offsets of less than 2 cm.

FRACTURE GEOMETRY AND MORPHOLOGY

The fractures that are the focus of this study are bed-normal and bed-parallel calcite veins. Although the veins are abundant in subsurface samples, they are uncommon in outcrops of the Nolichucky Shale due to pervasive groundwater flow and surface weathering effects (Dreier *et al.* 1988). Consequently, all fracture analysis was performed in approximately 500 m of unoriented 7.5 cm drill core from four wells with a maximum along-strike separation of 12 km. Fortunately, bed-normal vein orientations can be determined because bedding orientation is constant around the wells (Lemiszki & Hatcher 1990), and the core contains only rare faults and folds, and separates along bedding. Vein orientations are derived from true bedding orientation, core orientation from deviation logs (King & Haase 1987), apparent bedding dip value in the core, and pitch of the bed-normal vein trace on bedding (Fig. 2a). The apparent dip direction, pole to bedding and well pole are coplanar, and hence, plot on a great circle in an equal-area projection (Fig. 2a). The vein pitch on bedding is measured with respect to apparent strike and is corrected to true strike by projecting towards the center onto the true bedding trace. The pole to the actual vein orientation is 90° to the corrected pitch on the bedding trace.

Bed-normal veins occur in four prominent sets (Figs. 2b & c). When bedding is restored to the horizontal, strikes are 055° (parallel to present bedding strike), 320° (nearly perpendicular to present bedding strike), 015° and 090°. Kilsdonk & Wiltschko (1988) identified four similar sets in the Powell Valley anticline (Fig. 1a) of the Pine Mountain thrust sheet. They stated that the strike-parallel (055°) and strike-perpendicular (320°) sets are younger than the 015° and 090° sets from cross-cutting relationships and the absence of 015° and 090° veins in post-Ordovician rocks. By contrast, in the present study 35 bed-normal vein intersections in the cores show that the 015° and 090° sets mutually cross-cut the 055° and 320° sets (Table 1), so the four sets are coeval. Intersections have a simple morphology in which younger vein fill simply cuts and dilationally separates the older vein fill.

Bed-normal calcite veins are 0.5–2.0 mm wide, extend across the diameter of the drill core, and commonly cut across bedding contacts between shales and interbedded limestones. They contain equigranular ferroan calcite with subordinate quartz and ferroan dolomite. Rarely, the calcite is fibrous where the wall rock changes from oolitic limestone to calcareous siltstone. Wall-normal

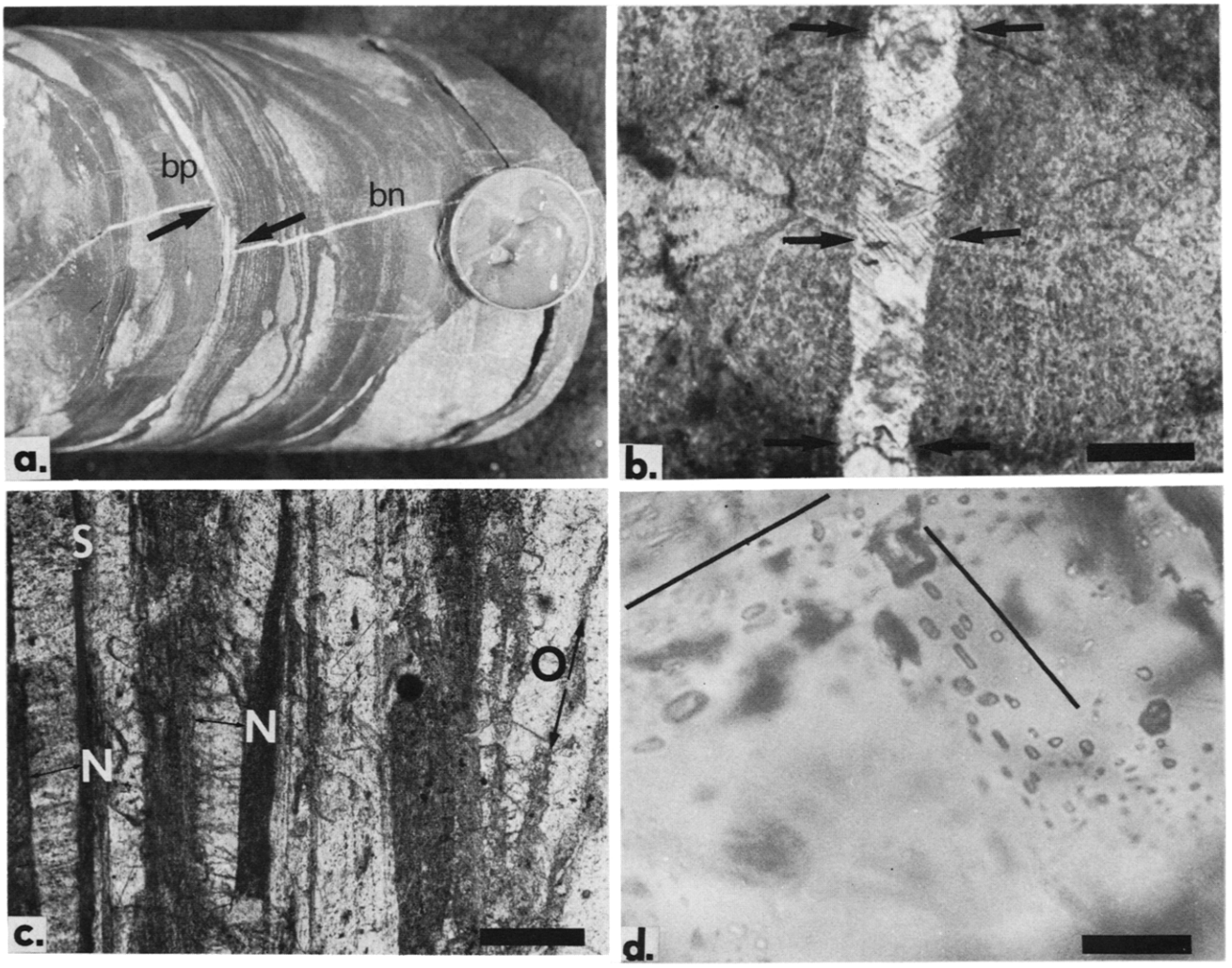

Fig. 3. Photographs showing mesoscopic and microscopic character of bed-normal and bed-parallel calcite veins. (a) Bed-normal vein (bn) offset by bed-parallel vein (bp) in drill core. Amount of offset shown by arrows, top of core towards coin (19 mm diameter). (b) Wall-normal displacement of fibrous calcite ooid by twinned equigranular bed-normal vein. Arrows match corresponding points on ooid separated by mode I fracture. Plane-polarized light. (c) Bed-parallel composite vein in shale showing wall-normal fibers (N), wall-oblique trails of shale wall fragments (O), and straight, sharp vein boundaries with clay minerals where bed-parallel slip was localized (S). Plane-polarized light. (d) Primary two-phase fluid inclusions along possible growth zones parallel to rhombohedral cleavage (bold lines) in uniformly dull luminescent calcite vein. Plane polarized light photograph of cleavage flake. Scale bars for (b) and (c) = 200 μm; for (d) = 100 μm.

Table 1. Relative ages of intersecting bed-normal vein sets from cross-cutting relationships

	Younger set			
Older set	015°	055°	090°	320°
015°	**	1	3	0
055°	0	**	3	6
090°	2	5	**	2
320°	5	6	2	**

displacements of ooids and fossils, and wall-normal fibers (Fig. 3b) indicate dilational mode I fracturing (Engelder 1982). Bed-normal veins are offset by bed-parallel slickensided veins in 49 out of 50 occurrences (Fig. 3a). Slickenside lineations are parallel to the Alleghanian thrusting direction (Fig. 2d), indicating that they formed during thrusting. Calcite within both bed-normal and bed-parallel veins is twinned (Fig. 3b) as a result of Alleghanian deformation (Wiltschko *et al.* 1985, Kilsdonk & Wiltschko 1988, Craddock & van der Pluijm 1989). Therefore, the four bed-normal sets are coeval mode I fractures that formed before local Alleghanian thrusting and calcite twinning.

Bed-parallel, slickensided calcite veins are present on bedding surfaces between limestones and shale, but also occur within shale. They are commonly less than 1 mm wide with fibrous slickenlines parallel to bedding dip on both vein margins. These multilayered veins have three calcite-grain textures in bed-normal slickenline-parallel profiles (Fig. 3c): (1) coarse, equant calcite fill; (2) long, layer-parallel fibrous crystals, with uniform extinction and straight boundaries against thin zones of fine-grained calcite and clay impurities, where bedding-parallel slip was concentrated (Stanley 1990); and (3) granular or layer-normal antitaxial fill transected by strongly oblique wall-rock fragments, indicting oblique dilation (Cox 1987). Consequently, the bed-parallel veins accommodated motions ranging from bed-parallel slip to wall-perpendicular dilation. Locally, younger oblique-pinnate veins containing granular calcite thicken the bed-parallel veins.

FLUID INCLUSIONS

Methods

Fluid inclusions from 12 oriented vein-bearing samples were examined in doubly polished thin sections prepared with slow speed diamond saws and polishing equipment. Inclusions in crystal cleavage flakes spalled from larger veins were also examined. Polished chips and unpolished flakes from the same veins had identical homogenization temperatures (T_h), demonstrating that chip preparation did not alter fluid inclusion characteristics.

The ease with which fluid inclusions in soft minerals such as calcite stretch, leak and decrepitate, requires steps to prevent inclusion deformation during microthermometric analysis (Prezbindowski & Larese 1987, Meunier 1989). Inclusion stretching increases inclusion volume by deformation of the host crystal whereas leaking inclusions partially lose fluid and decrepitated inclusions catastrophically lose all fluid. Stretched and leaked inclusions yield T_h values greater than undeformed inclusions, and decrepitated inclusions no longer contain fluid for microthermometric measurements.

The following steps were taken during microthermometric analysis to limit the possibility of unknowingly measuring deformed inclusions. First, only inclusions from the same field of view were measured at a time (generally three to five inclusions), before being replaced with a fresh chip from the same vein. By restricting measurements to inclusions within the same field of view, any sudden change in vapor/liquid ratios due to inclusion deformation could be observed, and removed from consideration. Second, heating runs were conducted before freezing runs to reduce the possibility of measuring homogenization temperatures of inclusions stretched by freezing (Meunier 1989). Third, only inclusions with maximum dimensions greater than about 15–20 μm were used for the freezing runs because they provided the most reproducible results. Microthermometric analyses were reproducible to within ±2°C. Repeat measurements were conducted with a blind over the thermocouple readout to limit observational bias.

Petrography

Liquid-rich two-phase (vapor + liquid) inclusions occur within bed-parallel and bed-normal calcite veins, have vapor/liquid ratios of 0.10–0.20, and do not contain daughter minerals. The maximum dimension of these inclusions ranges from less than 2 up to 90 μm and averages about 8 μm. Because of the cloudy nature of the calcite and small average inclusion size, considerable effort was required to find inclusions suitable for reproducible microthermometric measurements.

Primary inclusions are necessary to determine precipitation temperature, fluid salinity and composition during crystal growth. In contrast, pseudo-secondary and secondary inclusions indicate environmental and chemical conditions shortly following crystal growth, or substantially later, respectively. These conditions may be significantly different from those of initial crystal formation. Thus, differentiating primary and secondary inclusions is important, but an unequivocal primary origin for fluid inclusions is usually difficult to prove (Roedder 1984). Criteria for recognizing primary inclusions are occurrence of inclusions along crystal growth zones (Fig. 3d), negative crystal inclusion shape, random separation between adjacent inclusions, and the absence of inclusion trails cross-cutting crystal boundaries and growth zones (Roedder 1984). However, recrystallization of irregular primary inclusions into negative crystal-shaped secondary inclusions may occur to reduce surface free energy (Roedder 1984), so inclusion shape alone is insufficient to determine inclusion origin. In this study, primary (Fig. 3d) and definite secondary inclusions (forming curved or straight trails crossing crys-

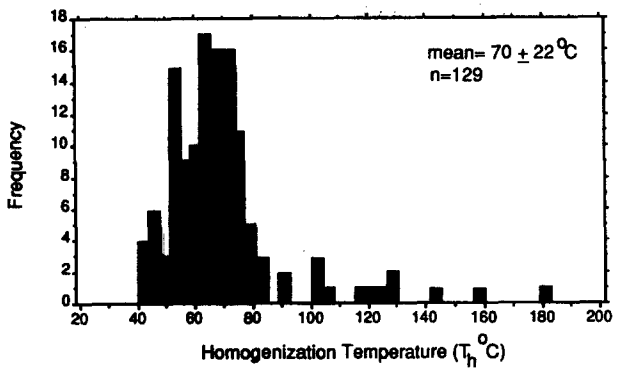

Fig. 4. Frequency histogram of homogenization temperatures for all bed-normal and bed-parallel veins.

Table 2. Fluid inclusion homogenization temperatures (T_h) from calcite veins in the Nolichucky Shale on the Oak Ridge Reservation (Whiteoak Mountain thrust sheet)

Vein orientation	Mean T_h	Median T_h	No. of inclusions
Bed-parallel	74.2 ± 34.8	61.1	31
Bed-normal	67.6 ± 16.8	68.5	95
055°	66.7 ± 10.9	67.4	69
320°	66.7 ± 10.9	68.4	27
015° and 090°	83.4 ± 24.3	83.7	6

tal boundaries), yielded identical T_h values and salinities, suggesting similar conditions during trapping of both inclusion classes. Uncertainties in differentiating between clearly primary and secondary inclusions are therefore less critical than in studies where significant differences in T_h and salinities exist between primary and secondary inclusions.

Heating runs

Results from the heating runs for bed-parallel and bed-normal veins show a single population clustered at $T_h = 70 \pm 22$°C (Fig. 4). No significant difference in T_h exists between bed-normal veins and bed-parallel veins (Table 2).

Freezing runs

The inclusion fluid composition can be estimated by observing the temperature at which phase changes occur during thawing of the inclusion from a frozen state (Roedder 1984). Inclusions required considerable undercooling (generally −70 to −90°C) before complete freezing, as is commonly the case for high salinity fluids. Freezing was marked by the migration of a brown color change across the inclusion, which is characteristic of NaCl–$CaCl_2$ fluids (Shepherd *et al.* 1985).

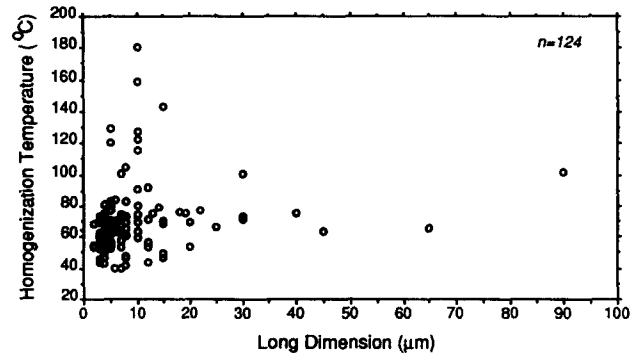

Fig. 5. Homogenization temperature vs maximum dimension for inclusions.

First melting or eutectic temperatures from inclusions in bed-parallel and bed-normal veins ranged from −57 to −48°C (mean $T_e = -50 \pm 6$°C, $n = 22$), corresponding to the temperature at which liquid first co-exists with other solids, such as ice and hydrous salts, during thawing. These temperatures are in agreement with published eutectic temperatures for the NaCl–$CaCl_2$–H_2O system (−55.0°C Borisenko 1977, −52.0°C Crawford 1981). With continued heating, the next phase transition was ice melting at a mean $T_m = -22 \pm 3$°C ($n = 28$). Further warming resulted in the melting of hydrohalite ($NaCl \cdot 2H_2O$) at a mean $T_m h = -8 \pm 4$°C ($n = 16$). Hydrohalite is distinguished from ice by its higher relief and tendency to remain fixed to the inclusion wall rather than the vapor bubble (Roedder 1984). Also, hydrohalite crystals are nearly volume-constant during temperature decrease, unlike ice crystals which rapidly increase in size. The sequential freezing method described by Haynes (1985) was used to determine T_m and $T_m h$.

Using a NaCl–$CaCl_2$–H_2O phase diagram, the average inclusion melting behavior indicates a mean fluid composition of 17.5 wt% NaCl and 9.5 wt% $CaCl_2$ (Crawford 1981, Shepherd *et al.* 1985). This composition is comparable to sedimentary basin formation waters given that some dissolved species in the inclusion fluid are unidentified or unquantified (Table 3).

Crushing stage test

Individual fluid inclusions from more than 50 vein calcite chips were crushed using an Exxon-type crushing stage to determine if gases other than water vapor were present and to determine inclusion vapor pressure relative to atmospheric pressure (Roedder 1972, 1984, Hanor 1987). Intact fluid inclusions at room temperature should have pressures of about 0.03 atm (Roedder 1984). Upon crushing, the vapor bubbles in these inclusions should collapse from the greater external atmospheric pressure. However, if the inclusions contain noncondensible gases such as CO_2 or CH_4, their vapor pressure may exceed 1 atm, and generate a stream of bubbles during crushing. The freezing runs for Nolichucky fluid inclusions demonstrated the absence of CO_2. Methane in fluid inclusions is detectable by crushing them in kerosene or glycerol; vapor bubbles of CH_4 will dissolve in kerosene (Roedder 1972, Hanor 1987), but are insoluble in glycerol and maintain constant size or undergo size increase following crushing. Vapor bubbles in fluid inclusions from Nolichucky calcite veins collapsed upon crushing and disappeared as either glycerol or kerosene displaced the fluid inclusion contents, which implies the absence of methane or other

Table 3. Calculated fluid composition in vein calcite fluid inclusions compared to Gulf Coast formation waters and east Tennessee MVT fluids

	Nolichucky*	Norphlet Fm†	Frio Fm‡	E. TN MVT§
TDS	327,500	326,400	105,000–280,000	245,300
Cl	206,500	198,700	20,000–152,000	150,400
Na	81,000	79,000	23,000– 40,000	59,000
Ca	40,000	34,000	10,000– 40,000	27,000
Na/Cl	0.60	0.61	0.54–1.39	0.60
Ca/Cl	0.17	0.15	0.23–0.44	0.16
Na/Ca	3.52	4.07	2.35–3.16	3.74
Na/TDS	0.24	0.24	0.14–0.22	0.23
Ca/TDS	0.11	0.10	0.10–0.14	0.11
Cl/TDS	0.65	0.61	0.1 –0.54	0.61
Σ/TDS	1.00	0.95	0.43–0.90	0.96

All concentrations are in mg l^{-1}. *X*/Cl expressed as mole ratios. *X*/TDS expressed as weight ratios. TDS = total dissolved solids. Σ/TDS = weight ratio (Na + Ca + Cl)/TDS.

*Nolichucky concentrations calculated from freezing behavior assuming concentrations of species other than NaCl and $CaCl_2$ are minimal. Nolichucky fluid density = 1.18 g ml^{-1}.

†Brine compositions from Carpenter *et al.* (1974).

‡Ca-rich brines of Morton & Land (1987).

§Inclusion fluid composition, high salinity sphalerite, Mascot, Jefferson City, from Kesler *et al.* (1989).

pressurized gases. The crushing tests also demonstrated that the inclusions have not leaked after uplift into the near-surface environment as they presently contain vapor pressures less than 1 atm at room temperature (Roedder 1984).

DISCUSSION

Pressure–temperature conditions during veining

With the exception of boiling fluids, homogenization temperatures underestimate inclusion trapping temperatures for fluids lacking methane saturation (Roedder 1984, Hanor 1987). The correction to the homogenization temperature depends on fluid pressure and density during fluid trapping (Roedder & Bodnar 1980, Roedder 1984). In this study, pressure corrections were determined by noting the *P–T* conditions at which a line of constant homogenization temperature (LOCHT), or constant fluid density curve intersected lithostatic and hydrostatic pressure curves on a *P–T* diagram (Fig. 6) (Zhang & Frantz 1987, Srivistava & Engelder 1990).

A unique *P–T* value can be estimated for bed-parallel veins because vertical dilation implies that fluid and lithostatic pressure were equal (Gretener 1979, Srivistava & Engelder 1990). Thus, bed-parallel veins formed at about 110°C and 90 MPa (3.6 km, Fig. 6). In contrast, bed-normal veins with horizontal dilation do not have this pressure constraint, therefore fluid pressure may have ranged from hydrostatic to lithostatic (Fig. 6). Trapping conditions for inclusions in bed-normal veins ranged from 80 to 110°C and 25 to 90 MPa (2.4–3.6 km, Fig. 6), and reflect the uncertainty in fluid pressure.

Timing of veining

The timing of vein formation with respect to depth, temperature, and burial rate was modeled using a

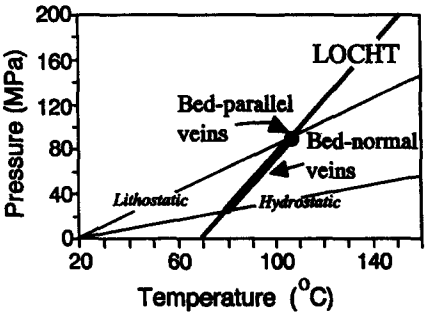

Fig. 6. *P–T* diagram used to calculate inclusion trapping temperatures. Bold line segment on line of constant homogenization temperature (LOCHT), indicates calculated *P–T* conditions for bed-normal vein formation. Circle at lithostatic–LOCHT intersection shows calculated *P–T* conditions for bed-parallel vein precipitation. LOCHT calculated from equation of state of Zhang & Frantz (1987) with T_h = 70°C, salinity = 27 wt% NaCl equivalent and density = 1.18 g ml^{-1}. Lithostatic = lithostatic pressure gradient (26 MPa km^{-1}); Hydrostatic = hydrostatic pressure gradient (10 MPa km^{-1}). Geothermal gradient assumed to be 25°C km^{-1}.

decompacted burial curve (Sclater & Christie 1980) for Middle Cambrian to Pennsylvanian strata (Fig. 7). Stratigraphic thicknesses in the Oak Ridge area were compiled from Hatcher *et al.* (1989) and State of Tennessee Division of Geology maps (Swingle & Luther 1964, Statler & Sykes 1970). The burial curve indicates temperatures experienced by the Nolichucky Shale, including inclusion trapping temperatures, which are assumed to be equal to ambient temperatures.

The reliability of this burial curve can be evaluated by comparing its predictions to time–temperature-sensitive indicators in the Nolichucky Shale and overlying rocks. Figure 7 predicts maximum burial temperatures of 75–90°C for Ordovician limestones (Och), which are consistent with conodont Color Alteration Index values (CAI = 1.5–2.0) from the limestones that indicate 60–110°C (Epstein *et al.* 1977, Harris 1979). Figure 7 also predicts maximum burial temperatures of 105–110°C for the Nolichucky Shale. Minerals of the lower to middle diagenesis zone (chlorite, kaolinite, mixed-layer illite/

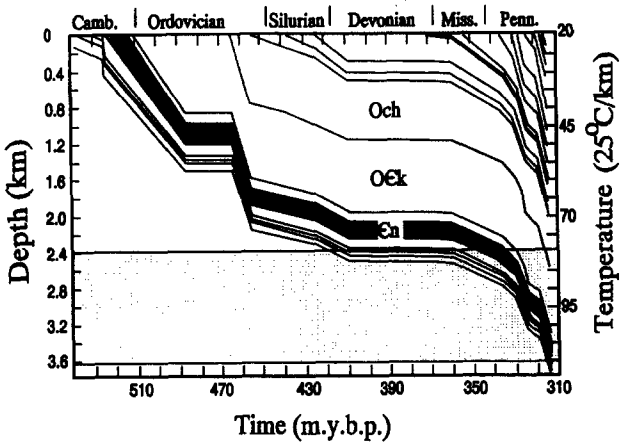

Fig. 7. Decompacted burial curve for the Conasauga Group and younger strata in the Whiteoak Mountain thrust sheet. Dark pattern = Nolichucky Shale; OЄk = Cambro–Ordovician Knox Group; Och = middle Ordovician Chickamauga Group. Stippled band indicates range of corrected inclusion temperatures. Plot constructed using Subside!© (Wilkerson & Hsui 1989).

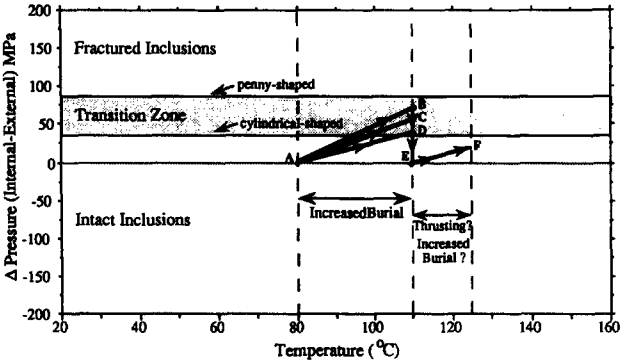

Fig. 8. Differential fluid pressure (ΔP) inside fluid inclusion relative to external confining pressure as a function of increasing ambient temperature. Bold lines mark possible burial trajectories for inclusions trapped at 80°C prior to thrusting. Line AB is for no increase in confining pressure. Line AC is where increase in confining pressure is hydrostatic, line AD is where increase in confining pressure is lithostatic. Transition zone defines range of ΔP required to cause brittle deformation for 8 μm inclusions as a function of shape variation (Lacazette 1990, Lacazette unpublished data).

smectite with 20–30% smectite layers, and glauconite) are present in the underlying Pumpkin Valley Shale (Lee *et al.* 1987) and indicate maximum burial temperatures of about 90–200°C (Weaver 1984). Also, illite crystallinity values (Weaver Index = 1.2) from these shales suggest maximum burial temperatures of less than 150°C (Weaver 1984, p. 192). The correlation of predicted temperatures with available time–temperature indicators supports the burial curve as being appropriate for modeling ambient temperatures during burial. It also demonstrates that the maximum sedimentary burial of the Nolichucky Shale was probably reached prior to thrusting.

Ambient burial temperatures for the Nolichucky Shale (Fig. 7) reached fluid inclusion trapping temperatures in bed-normal veins after the Middle Mississippian. Thus, bed-normal veins developed after 350 Ma B.P. and as much as 65 Ma prior to local Alleghanian thrusting (Secor *et al.* 1986). However, similar fluid chemistries for bed-normal and bed-parallel vein inclusions indicate the two vein types precipitated from nearly identical fluids at similar times, probably shortly before local Alleghanian thrusting.

Post-entrapment changes to fluid inclusions

Inclusions in calcite can stretch, leak or decrepitate in response to differential stress across the host crystal in excess of crystal strength (Prezbindowski & Larese 1987, Goldstein 1986, Burruss 1987, Meunier 1989, Lacazette 1990). Similar behavior has been recognized in other relatively soft minerals including barite, fluorite, and sphalerite (Bodnar & Bethke 1984, Ulrich & Bodnar 1988). Inclusion stretching or leaking can result from heating of the inclusion fluid beyond T_h, which increases internal fluid pressure and causes inclusion failure by brittle deformation (Prezbindowski & Larese 1987, Ulrich & Bodnar 1988, Burruss 1989, Meunier 1989). Geologic causes for temperature increases above T_h include additional burial after trapping by deposition or thrust loading. Several experimental studies demonstrate that if such heating and deformation occur, inclusion populations exhibit a positive correlation between inclusion size and homogenization temperature (Bodnar & Bethke 1984, Prezbindowski & Larese 1987). In this study, relatively tight clustering of T_h values about a single mode (Fig. 4), and the lack of correlation between inclusion size and T_h (Fig. 5) indicate that the measured inclusions have not re-equilibrated by stretching or leaking.

In addition to the petrographic and microthermometric evidence that indicate the fluid inclusions did not suffer post-entrapment re-equilibration, a simple worst-case mechanical analysis (Lacazette 1990) also supports this interpretation. This approach maximizes the pressure differential ($\Delta P = P_{\text{internal fluid}} - P_{\text{external confining}}$) across the host crystal that results from post-entrapment heating by assuming a minimum external confining pressure, and determines if ΔP is large enough to deform the inclusions by brittle failure. This analysis was applied to inclusions of similar size and shape (8 μm mean maximum dimension) to those studied here (Fig. 5).

The greatest internal fluid pressure increase due to heating is achieved by assuming that the inclusion formed at a minimum trapping temperature of 80°C (Fig. 6), and was then subjected to additional burial of 1.5 km to reach an ambient temperature of 110°C (Fig. 7), which corresponds to temperatures of bed-parallel veining and thrusting. In the worst-case analysis, the external confining pressure does not counteract the increase in internal fluid pressure. Therefore, a maximum differential pressure of 73 MPa is given by the slope of the 27 wt% isochore for $\Delta T = 30$°C (110–80°, Figs. 6 and 8). As shown in Fig. 8, the ΔP–T trajectory (line AB) exceeds the value of ΔP for brittle failure of some inclusions but is insufficient to deform penny-shaped inclusions (Lacazette 1990). This analysis indicates that differential pressures were probably not of sufficient magnitude to cause brittle failure of inclusions

in Nolichucky calcite veins prior to thrusting. Under more realistic and less extreme conditions, the least confining pressure would increase with burial and thereby reduce ΔP. The increase in confining pressure may range from hydrostatic to lithostatic (lines AC and AD, Fig. 8), which would result in significantly lower differential pressure compared to the worst-case scenario. During thrusting, the least confining pressure would equal the vertical lithostatic load and thereby substantially reduce ΔP (line BEF).

The worst-case analysis indicates that deformation of Nolichucky vein calcite inclusions by brittle failure is unlikely; under more realistic conditions the possibility for inclusion deformation is even less. Such conditions include: (1) bed-normal veins were probably trapped at temperatures similar to bed-parallel veins (100–110°C rather than 80°C) as indicated by similar fluid chemistries; (2) confining pressure must have increased during additional burial unless the host calcite had a Poisson's ratio and thermal expansivity of zero (Haxby & Turcotte 1976, Dunne 1986), which is not the case (Handin 1966); and (3) the increase in minimum confining pressure to approach lithostatic pressure with the onset of thrusting was probably gradational, rather than instantaneous as shown in Fig. 8 (line BE), and would have reduced the differential pressure to values less than those at points B, C and D in Fig. 8. Incorporation of these conditions into a more sophisticated analysis is beyond the scope of this paper.

Possible causes for coeval bed-normal vein sets

Cross-cutting relationships, fracture geometry, fluid inclusions and a decompacted burial curve, show that four bed-normal vein sets in the WOM cores formed: (1) coevally during similar thermal conditions and from similar fluids; (2) after the middle Mississippian; and (3) before bed-parallel veins developed during local thrusting. In this time frame, bedding would have been nearly horizontal, and bed-normal veins would have formed vertically.

Coeval pairs of orthogonal vertical mode I fracture sets can form when the horizontal principal stresses are nearly hydrostatic (Price 1967, Pollard & Aydin 1988, Dunne & North 1990). Small fluctuations in remote stresses, or local stress changes as a result of deformation such as flexure during passage of a peripheral bulge, can trigger orthogonal fracturing. Fracture propagation in one direction releases stress, 'flip-flopping' the horizontal principal stresses and triggering the propagation of the orthogonal set (Price 1967). However, this mechanism only produces two coeval fracture sets. The existence of four coeval bed-normal mode I vein sets requires that the regional minimum principal stress fluctuated between four different horizontal directions, which requires the interaction of a combination of structures or far-field stress components. At Oak Ridge, the tectonic setting after the middle Mississippian and before the onset of local thrusting could have formed the basis for such an interaction, as the area was proximal to two coeval and non-parallel thrust systems, the Ouachita and Alleghanian (Fig. 9).

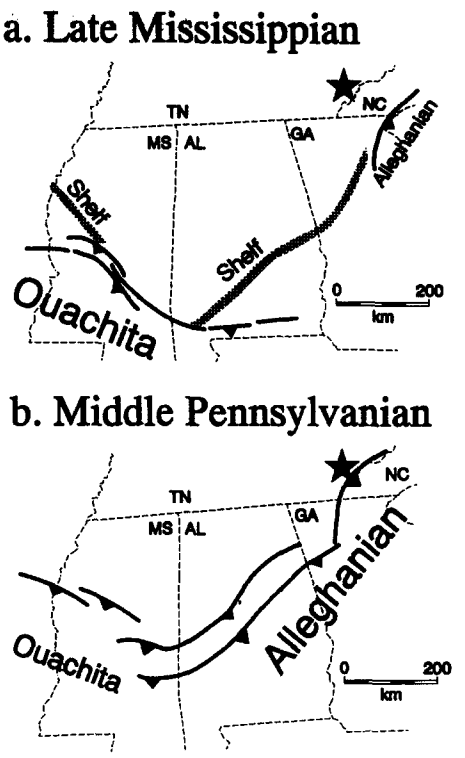

Fig. 9. (a) Reconstruction of Ouachita and Alleghanian orogenic belts (thrust fault symbols) in the late Mississippian. (b) Middle Pennsylvanian, the Alleghanian orogenic system has encroached on the Oak Ridge area. Modified from Thomas (1990).

For a single thrust system, coeval vertical mode I fractures beyond the system are commonly parallel and perpendicular to structural trend (Stauffer & Gendzwill 1987, Dunne & North 1990). In the two thrust-system case, the 055° and 320° vein sets are parallel and perpendicular to local Alleghanian structural trend, whereas 015° and 090° sets are subperpendicular and parallel to the nearest portion of the Ouachita thrust system. Thus, the fracture trends are consistent with an interpretation where fluctuation between the two orogenic compressions generated four coeval vertical fracture sets beyond the limits of thrusting. This interpretation is, however, speculative because it is inferred from a small region, and the 015° and 090° sets are not ideally orthogonal with respect to the Ouachita thrust system. If this interpretation is correct, the interaction probably occurred just in advance of local thrusting because fluid inclusions in bed-normal and bed-parallel veins suggest similar trapping conditions and fluid chemistries.

CONCLUSIONS

Within the Nolichucky Shale, the Whiteoak Mountain thrust sheet contains four bed-normal vein sets that predate both bed-parallel slickensided veins and emplacement of the WOM sheet. Restoring bedding to a pre-thrusting attitude, the bed-normal vein sets were oriented 015°, 055° (regional strike direction), 090° and 320° (sub-perpendicular to regional strike).

Fluid inclusions indicate that bed-normal veins precipitated at temperatures of 80–110°C, and at depths of 2.4–3.6 km from highly saline NaCl–$CaCl_2$ brines. Bed-parallel veins formed during maximum burial at 110°C, and 3.6 km depth, from brines of similar composition and salinity as the bed-normal veins. Fluid inclusions in the bed-normal and bed-parallel calcite veins formed near maximum sedimentary burial depths and were not sufficiently overheated to cause brittle failure during additional burial or thrusting.

Fluid inclusions and a decompacted Nolichucky burial curve suggest that bed-normal veins formed after the middle Mississippian during the onset of the Ouachita and Alleghanian orogenies, but prior to bed-parallel slickensided veins that formed during movement of the WOM sheet. The similarity in the compositions of fluids that precipitated both bed-normal and bed-parallel veins suggests the bed-normal veins formed immediately prior to thrusting and formation of the bed-parallel veins. The development of four bed-normal vein sets could have been controlled by far-field compressive stresses interacting between the two orogenies.

Acknowledgements—This work was supported by a U.S. Department of Energy Oak Ridge National Laboratory doctoral fellowship to J. L. Foreman under the helpful supervision of dissertation advisor K. R. Walker (UT) and G. K. Jacobs (ORNL). Additional support for J. L. Foreman was provided by the D.O.E. Oak Ridge Reservation Hydrologic and Geologic Studies Program, Geological Society of America, Sigma Xi, Appalachian Basin Industrial Associates, the University of Tennessee Geological Sciences Discretionary Fund, and the Carbonate Research Fund. Constructive reviews and valuable assistance came from Alfred Lacazette, R. D. Hatcher, R. B. Dreier and P. J. Lemiszki. Comments from an anonymous reviewer and members of J. L. Foreman's dissertation committee are also appreciated, but the conclusions presented here remain the responsibility of the authors.

REFERENCES

Beaumont, C. 1981. Foreland basins. *Geophys. J. R. astr. Soc.* **65**, 291–329.

Beaumont, C., Quinlan, G. & Hamilton, J. 1988. Orogeny and stratigraphy: numerical models of the Paleozoic in the eastern interior of North America. *Tectonics* **7**, 389–416.

Bodnar, R. J. & Bethke, P. M. 1984. Systematics of stretching of fluid inclusions I: Fluorite and sphalerite at 1 atmosphere confining pressure. *Econ. Geol.* **79**, 141–161.

Borisenko, A. S. 1977. Study of the salt composition of gas-liquid inclusions in minerals by the cryometric method. *Soviet Geol. & Geophys.* **18**, 11–19.

Burruss, R. C. 1987. Diagenetic paleotemperatures from aqueous fluid inclusions: Re-equilibration of inclusions in carbonate cements by burial heating. *Mineralog. Mag.* **51**, 477–481.

Burruss, R. C. 1989. Paleotemperatures from fluid inclusions: Advances in theory and technique. In: *Thermal History of Sedimentary Basins* (edited by Naeser, N. D. & McCulloh, T. H.). Springer, New York, 119–132.

Carpenter, A. B., Trout, M. L. & Pickett, E. E. 1974. Preliminary report on the origin and chemical evolution of lead- and zinc-rich oil field brines in central Mississippi. *Econ. Geol.* **69**, 1191–1206.

Cox, S. F. 1987. Antitaxial crack–seal vein microstructures and their relationship to displacement paths. *J. Struct. Geol.* **9**, 779–787.

Craddock, J. P. & van der Pluijm, B. A. 1989. Late Paleozoic deformation of the cratonic carbonate cover of eastern North America. *Geology* **17**, 416–419.

Crawford, M. L. 1981. Phase equilibria in aqueous fluid inclusions. In: *Short Course in Fluid Inclusion* (edited by Hollister, L. S. & Crawford, M. L.). *Applic. Petrol. Miner. Ass. Can.* **6**, 75–100.

Dreier, R. B., Lutz, C. T., Toran, L. E. & Bittner, E. 1988. Fracture and hydraulic conductivity investigations in a complex low-permeability geologic environment (Abs.). Conf. on Flow and Transport in Low-permeability Settings, Nat. Water Well Assoc.

Dunne, W. M. 1986. Mesostructural development in detached folds: an example from West Virginia. *J. Geol.* **94**, 473–488.

Dunne, W. M. & North, C. P. 1990. Orthogonal fracture systems at the limits of thrusting: an example from southwestern Wales. *J. Struct. Geol.* **12**, 207–215.

Engelder, T. 1982. Reply to a comment on "Is there a genetic relationship between selected regional joints and contemporary stress within the lithosphere of North America" by A. E. Scheidegger. *Tectonics* **1**, 465–470.

Engelder, T. 1985. Loading paths to joint propagation during a tectonic cycle: an example from the Appalachian Plateau, U.S.A. *J. Struct. Geol.* **7**, 459–475.

Epstein, A. G., Epstein, J. B. & Harris, L. D. 1977. Conodont color alteration—an index to organic metamorphism. *Prof. Pap. U.S. geol. Surv.* **995**.

Fleming, P. B. & Jordan, T. E. 1989. A synthetic stratigraphic model of foreland basin development. *J. geophys. Res.* **94**, 3851–3866.

Goldstein, R. H. 1986. Reequilibration of fluid inclusions in low-temperature calcium–carbonate cement. *Geology* **14**, 792–795.

Gretener, P. E. 1979. Pore pressure: Fundamentals, general ramifications and implications for structural geology. *Am. Ass. Petrol. Geol. Continuing Education Course Note Ser.* **4**.

Hancock, P. L. 1985. Brittle microtectonics: principles and practice. *J. Struct. Geol.* **7**, 437–457.

Hancock, P. L. & Engelder, T. 1989. Neotectonic joints. *Bull. geol. Soc. Am.* **101**, 1289–1305.

Handin, J. 1966. Strength and ductility. In: *Handbook of Physical Constants* (edited by Clark, S. P.). *Mem. geol. Soc. Am.* **97**, 223–290.

Hanor, J. S. 1987. *Origin and Migration of Subsurface Sedimentary Brines. Soc. Econ. Petrol. Miner. Short Course Notes* **21**.

Harris, A. G. 1979. Conodont color alteration, an organo-mineral metamorphic index, and its application to Appalachian Basin geology. In: *Aspects of Diagenesis* (edited by Scholle, P. A. & Schluger, P. R.). *Spec. Publ. Soc. econ. Petrol. Miner.* **26**, 3–16.

Hatcher, R. D., Jr., Ketelle, R. H., Lee, R. R., Lemiszki, P. J. & McMaster, W. M. 1989. Field guide and perspective on the geology and hydrology of the Oak Ridge Reservation. Unpublished field guidebook.

Haxby, W. F. & Turcotte, D. L. 1976. Stress induced by the addition or removal of overburden and associated thermal effects. *Geology* **4**, 181–185.

Haynes, F. M. 1985. Determination of fluid inclusion compositions by sequential freezing. *Econ. Geol.* **80**, 1436–1439.

Jordan, T. E. 1981. Thrust loads and foreland basin evolution, Cretaceous, western United States. *Bull. Am. Ass. Petrol. Geol.* **65**, 2506–2520.

Kesler, S. E., Gesink, J. A. & Haynes, F. M. 1989. Evolution of mineralizing brines in the east Tennessee Mississippi Valley-type ore field. *Geology* **17**, 466–469.

Kilsdonk, B. & Wiltschko, D. V. 1988. Deformation mechanisms in the southeastern ramp region of the Pine Mountain block, Tennessee. *Bull. geol. Soc. Am.* **100**, 653–664.

King, H. L. & Haase, C. S. 1987. Subsurface controlled geologic maps for the Y-12 Plant and adjacent areas of Bear Creek Valley. ORNL/TM-10112, Oak Ridge National Laboratory, Martin Marietta Energy Systems.

Lacazette, A. 1990. Application of linear elastic fracture mechanics to the quantitative evaluation of fluid inclusion decrepitation. *Geology* **18**, 782–785.

Lee, S. Y., Hyder, L. K. & Alley, P. D. 1987. Mineralogical characterization of selected shales in support of nuclear waste repository studies. ORNL/TM-10567, Oak Ridge National Laboratory, Martin Marietta Energy Systems.

Lemiszki, P. J. & Hatcher, R. D. 1990. Contrasting structural geometries between the Whiteoak Mountain and Copper Creek thrust faults, Bethel Valley Quadrangle, east TN. *Geol. Soc. Am. Abs. w. Prog.* **22**, 23.

Meunier, J. D. 1989. Assessment of low-temperature fluid inclusions in calcite using microthermometry. *Econ. Geol.* **84**, 167–170.

Milici, R. C. 1970. The Alleghanian structural front in Tennessee and its regional tectonic implications. *Am. J. Sci.* **268**, 127–141.

Morton, R. A. & Land, L. S. 1987. Regional variations in formation water chemistry, Frio Formation (Oligocene), Texas Gulf Coast. *Bull. Am. Assoc. Petrol. Geol.* **71**, 191–206.

Nickelsen, R. P. & Hough, V. D. 1967. Jointing in the Appalachian Plateau of Pennsylvania. *Bull. geol. Soc. Am.* **78**, 609–630.

Pollard, D. D. & Aydin, A. 1988. Progress in understanding jointing over the past century. *Bull. geol. Soc. Am.* **100**, 1181–1204.

Prezbindowski, D. R. & Larese, R. E. 1987. Experimental stretching of fluid inclusions in calcite—Implications for diagenetic studies. *Geology* **15**, 333–336.

Price, N. J. 1967. *Fault and Joint Development in Brittle and Semi-brittle Rock.* Pergamon Press, Oxford.

Price, R. A. 1967. The tectonic significance of mesoscopic subfabrics in the southern Rocky Mountains of Alberta and British Columbia. *Can. J. Earth Sci.* **4**, 39–70.

Rich, J. L. 1934. Mechanics of low-angle overthrust faulting as illustrated by Cumberland thrust block, Virginia, Kentucky, and Tennessee. *Bull. Am. Ass. Petrol. Geol.* **18**, 1584–1596.

Rodgers, J. 1949. Evolution of thought on structure of middle and southern Appalachians. *Bull. Am. Ass. Petrol. Geol.* **33**, 1643–1654.

Roedder, E. 1972. Composition of Fluid Inclusions. In: *Data of Geochemistry* (edited by Fleischer, M.). *Prof. Pap. U.S. geol. Surv.* **440-JJ**.

Roedder, E. 1984. Fluid inclusions. *Rev. Mineral.* **12**.

Roedder, E. & Bodnar, R. J. 1980. Geologic pressure determinations from fluid inclusion studies. *Annu. Rev. Earth & Planet. Sci.* **8**, 263–301.

Sclater, J. C. & Christie, P. A. F. 1980. Continental stretching: An explanation of the post-mid-Cretaceous subsidence of the Central North Sea Basin. *J. geophys. Res.* **85**, 3711–3739.

Secor, D. T., Jr., Snoke, A. W. & Dallmeyer, R. D. 1986. Character of the Alleghanian orogeny in the southern Appalachians: Part III. Regional tectonic relations. *Bull. geol. Soc. Am.* **97**, 1345–1353.

Shepherd, T. J., Rankin, A. J. & Alderton, D. H. M. 1985. *A Practical Guide to Fluid Inclusion Studies.* Blackie & Sons, Glasgow.

Srivastava, D. C. & Engelder, T. 1990. Crack-propagation sequence and pore-fluid conditions during fault-bend folding in the Appalachian Valley and Ridge, central Pennsylvania. *Bull. geol. Soc. Am.* **102**, 116–128.

Stanley, R. S. 1990. The evolution of mesoscopic imbricate thrust faults— an example from the Vermont Foreland, U.S.A. *J. Struct. Geol.* **12**, 227–241.

Statler, A. T. & Sykes, C. R. 1970. Geologic Map and Mineral Resources Summary of the Duncan Flats Quadrangle, Tennessee. Tenn. Dept. Conserv., Div. Geol., GM 129-NE and MRS 129-NE, Nashville.

Stauffer, M. R. & Gendzwill, D. J. 1987. Fractures in the northern plains, stream patterns, and midcontinent stress field. *Can. J. Earth Sci.* **24**, 1086–1097.

Stockmal, G. S., Beaumont, C. & Boutilier, R. 1986. Geodynamic models of convergent margin tectonics: Transition from rifted margin to overthrust belt and consequences for foreland-basin development. *Bull. Am. Ass. Petrol. Geol.* **70**, 181–190.

Swingle, G. D. & Luther, E. T. 1964. Geologic Map and Mineral Resources Summary of the Clinton Quadrangle, Tennessee. Tenn. Dept. Conserv., Div. Geol., GM 137-SW and MRS 137-SW, Nashville.

Thomas, W. A. 1990. The Appalachian-Ouachita orogen beneath the Gulf Coastal Plain between the outcrops in the Appalachian and Ouachita Mountains. In: *The Appalachian Ouachita Orogen in the United Stated* (edited by Hatcher, R. D., Jr., Thomas, W. A. & Viele, G. W.). *The Geology of North America* **F-2**, 537–554.

Ulrich, M. R. & Bodnar, R. J. 1988. Systematics of stretching of fluid inclusions II: Barite at 1 atmosphere confining pressure. *Econ. Geol.* **83**, 1037–1046.

Weaver, C. E. 1984. *Shale–Slate Metamorphism in Southern Appalachians. Develop. Petrol.* **10**.

Wilkerson, M. S. & Hsui, A. T. 1989. *Subside!, A Basin Analysis Program.*

Wiltschko, D. V., Medwedeff, D. A. & Milson, H. E. 1985. Distribution and mechanisms of strain within rocks on the northwest ramp of Pine Mountain block, southern Appalachian foreland: A field test of theory. *Bull. geol. Soc. Am.* **96**, 426–435.

Woodward, N. B. 1985. Balanced cross-sections for the central and southern Appalachians. *Univ. Tennessee, Dept Geol. Sci., Stud. Geol.* **12**.

Zhang, Y. & Frantz, J. D. 1987. Determination of the homogenization temperature and densities of supercritical fluids in the system NaCl–KCl–$CaCl_2$–H_2O using synthetic fluid inclusions. *Chem. Geol.* **64**, 335–350.